Continuous-wave diode-pumped operation of an Yb:NaLa(WO$_4$)$_2$ laser at room temperature

Junhai Liu[a], José María Cano-Torres[b], Fátima Esteban-Betegón[b], María Dolores Serrano[b],

Concepción Cascales[b], Carlos Zaldo[b], Mauricio Rico[a], Uwe Griebner[a], Valentin Petrov[a],

[a]Max-Born-Institute for Nonlinear Optics and Ultrafast Spectroscopy,

2A Max-Born-Str., D-12489 Berlin, Germany

[b]Instituto de Ciencia de Materiales de Madrid, CSIC,

c/ Sor Juana Inés de la Cruz 3, Cantoblanco, E-28049 Madrid, Spain

Room-temperature continuous-wave (cw) laser operation is demonstrated with the newly developed Yb:NaLa(WO$_4$)$_2$ disordered crystal by end-pumping with a fiber-coupled diode laser. A maximum output power of 330 mW is obtained with an optical efficiency of 4.9% and a slope efficiency of 6.3% with respect to the incident pump power. The efficiencies in terms of the absorbed pump power are roughly three times higher. Sellmeier dispersion curves for the ordinary and extraordinary refractive indices of the NaLa(WO$_4$)$_2$ host are reported along with crystallographic and spectroscopic properties related to the Yb^{3+}-doping.

Key words: ytterbium lasers, sodium tungstate crystals, diode-pumped lasers

_____

Corresponding author: Dr. V. Petrov

Tel: +49-30-63921272, Fax: +49-30-63921289, E-mail: petrov@mbi-berlin.de

1. Introduction

Monoclinic potassium double tungstates including $KY(WO_4)_2$, $KGd(WO_4)_2$, and more recently $KLu(WO_4)_2$, represent one of the most important groups of laser host materials for the ytterbium ion. Such Yb-doped crystals, characterized by their large absorption and emission cross sections, have found wide applications in diode-pumped lasers and particularly in femtosecond laser technology. In contrast to the above mentioned potassium based double tungstates, sodium double tungstates, $NaT(WO_4)_2$, where T=Bi, Y, La, or rare earth Ln, are uniaxial and possess a tetragonal crystallographic structure. The crystals belonging to this group are usually called "disordered" because Na^+ and T^{3+} ions share almost randomly the same lattice sites. In comparison to the "ordered" monoclinic double tungstates, the laser active Ln^{3+} absorption and emission bands are found to be broadened as a result of the inhomogeneous crystal field induced by this random distribution [1,2]. Therefore, Yb-doped disordered double tungstates could be more promising in generating femtosecond laser pulses by passive mode-locking techniques in comparison to the currently used monoclinic potassium tungstates.

Unlike the Yb-doped monoclinic tungstates that have been studied extensively since the late 90's, the investigation of Yb-doped tetragonal sodium tungstates has just begun. So far, lasing has been demonstrated only in two such crystals: $Yb:NaGd(WO_4)_2$ [3,4] and $Yb:NaLa(WO_4)_2$ (Yb:NaLaW) [5]. For Yb:NaLaW, laser operation with a maximum output power of 205 mW was reported only under Ti:sapphire laser pumping [5]. However, for widespread applications the present photonic technology requires the use of diode pumping. In this work, we investigate the cw laser performance of an Yb:NaLaW crystal end-pumped

by a fiber-coupled diode laser and provide basic optical properties of the host and Yb^{3+} spectroscopy.

2. Crystal preparation and optical host properties

Yb-doped NaLaW crystals were grown by the Czochralski method. Details of the crystal growth can be found elsewhere [6]. Transparent samples were obtained for ytterbium concentrations up to 4 wt% (15.4 mol%) in the melt. Up to this doping level micrometer-size bubbles occasionally appear locally but for higher levels the density of these defects increases with Yb concentration. The tetragonal structure was confirmed by X-ray diffraction and it was established that the Yb incorporation leads to reduction of the unit cell parameters a and c according to the dependences $a=5.3552-0.1173x$ (Å) and $c=11.667-0.334x$ (Å), where $x=0\ldots0.2$ is the molar ytterbium concentration in the crystal, i.e. $NaLa_{1-x}Yb_x(WO_4)_2$. These results have been obtained using a W standard ground and mixed with the analyzed single crystals, and possess therefore much higher accuracy than previous NaLaW lattice cell parameter determinations [7-9].

Earlier studies indicated NaLaW transparency extending from ≈380 nm to ≈10 μm [10]. This same work also reported the room temperature values of the refractive indices in the wavelength range 691-472 nm: $n_o=$ 1.94-1.95 (±0.01) and $n_e=1.95-1.98$ (±0.01). We have revised these optical properties and found that the ultraviolet absorption is anisotropic. The short-wave absorption edges are at about 312 and 316 nm for the π and σ polarizations, respectively. The crystal birefringence is smaller than previously reported, namely $\Delta n<0.005$. NaLaW exhibits an isotropic point, changing from slightly positive to negative uniaxial near

546 nm (Fig. 1). The dispersion of the refractive indices has been fitted to single-pole Sellmeier equations containing an infrared correction term: $n^2 = A + \dfrac{B}{1 - \left(\frac{C}{\lambda}\right)^2} - D\lambda^2$. The parameters A, B, C and D obtained from the fit are summarized in Fig. 1.

Due to the quasi-three-level operation of ytterbium lasers a large enough crystal field splitting of the $^2F_{7/2}$ ground and $^2F_{5/2}$ excited manifolds is required. In order to quantify this effect we determined the Yb^{3+} Stark levels by 5 K optical absorption and luminescence measurements. The energy levels are $^2F_{7/2}$: 0, 177, 328 , 462 cm^{-1} and $^2F_{5/2}$: 10271, 10356, 10645 cm^{-1}. Therefore, the crystal field splitting in NaLaW is similar to that found in other Yb laser crystal hosts and comparable to the splitting in $KY(WO_4)_2$ and $KGd(WO_4)_2$ [11].

The ground state optical absorption cross section σ_{GSA} of Yb^{3+} in NaLaW has been presented previously for unpolarized [12] and polarized light [5]. The Yb^{3+} optical absorption in NaLaW exhibits a dichroic character. Averaging results obtained with different samples we obtained the following updated peak values: σ_{GSA}^{π} (λ=976.2 nm)= $1.60\pm0.1\times10^{-20}$ cm^2 and σ_{GSA}^{σ} (λ=975.9 nm)= $1.15\pm0.1\times10^{-20}$ cm^2. The corresponding peak emission cross sections calculated by the reciprocity method are: σ_{em}^{π} (λ=976.2 nm)= $1.78\pm0.1\times10^{-20}$ cm^2 and σ_{em}^{σ} (λ=975.9 nm)= $1.25\pm0.1\times10^{-20}$ cm^2. The upper level lifetime of Yb:NaLaW estimated in [6] for low Yb-doping levels amounts to 220 μs.

3. Experimental laser setup

The Yb:NaLaW sample used in laser experiments was an uncoated *a*-cut plate, with a thickness of 3.4 mm. The Yb concentration in the crystal was 1.1×10^{20} cm^{-3} ($\approx$3 mol%). Fig. 2 shows a schematic diagram of the experimental laser setup. A nearly hemispherical

cavity was used to take advantage of the small mode size for reduction of the reabsorption losses in the gain medium inherent to quasi-three-level systems like Yb lasers. M_1 was a plane mirror, its rear surface was anti-reflection coated for 980 nm, while the front surface was highly reflecting for 1020-1200 nm and highly transmitting near 980 nm. M_2 was a 50-mm-radius-of-curvature concave output coupler. Four different mirrors with transmission T=0.5%, 1%, 2%, and 3% at 1030 nm were used. The Yb:NaLaW crystal was mounted on a copper holder that was not actively cooled, and placed as close as possible ($\approx$0.2 mm) to the end mirror M_1. The pump source used was a fiber-coupled diode laser module (fiber: 116 μm core diameter, 0.2 NA, Boston Laser, Inc.). Its unpolarized output was focused by f=6.2 mm microoptics (Schäfter&Kirchhoff) through the 3 mm thick quartz substrate of M_1 to a spot size of $\approx$40 μm (waist) in the position of the Yb:NaLaW crystal in order to match the fundamental laser mode size. The maximum available pump power measured after the focusing microoptics amounted to 7 W for a central wavelength near 978 nm.

4. Laser operation results and discussion

Operation of the diode-end-pumped Yb:NaLaW laser in the cw regime was possible using all four output couplers of 0.5-3% transmission. The output laser beam was found to be linearly π-polarized, this is due to the fact that the effective gain cross section is larger for this polarization. The lasing wavelength varied with the output coupling, decreasing from 1036.2 to 1026.2 nm when the transmission was increased from T=0.5% to 3%, a typical behaviour observed in Yb lasers. It has been demonstrated that the Yb:NaLaW laser is tunable in a wide range from 1017 to 1057 nm if a suitable tuning element is used [5].

Fig. 3 shows the dependence of the output power on the incident pump power for different output couplers. In the present laser configuration it was not possible to measure the absorbed pump power under lasing conditions because of the high divergence of the focused pump beam. A maximum output power of 330 mW was obtained at the highest available pump power of 6.8 W (incident on the crystal) when the 1% output coupler was used, giving an optical conversion efficiency of 4.9%, while the slope efficiency for the same output coupler amounted to 6.3%.

We measured the absorbed pump power in the crystal under non-lasing conditions. Fig. 4 gives the variation of the absorption (the ratio of absorbed pump power to incident pump power) with the incident pump power. The absorption was quite low, ranging from 0.28 to 0.34. This is attributed to the low doping level of the used crystal, which corresponds to an absorption coefficient (π-polarization) of 1-1.9 cm^{-1} for the wavelength range 970-980 nm. As can be seen from Fig. 4 the bleaching was almost absent in the case of diode pumping in contrast to Ti:sapphire laser pumping [5] where the narrow band pump radiation is adjusted to the absorption peak and the averaged (over the crystal length) pump intensity is higher. It is worth mentioning that the absorption measured without lasing is actually lower than the absorption when the laser operates due to the "recycling effect" of the ground manifold population caused by the circulating intracavity laser intensity but this effect tends to restore the small signal absorption value [13, 14]. If we assume a constant absorption of 30%, the actual slope efficiency will amount to ≈20%, this is comparable to the results obtained very recently with a diode-pumped Yb:NaGd(WO$_4$)$_2$ laser based on a similar cavity, that generated a maximum output power of 227 mW with a slope efficiency of 19.6% calculated with

respect to the absorbed pump power [4].

At the laser threshold no recycling effect exists because of the negligible intracavity laser field and the estimated threshold absorbed power measured without lasing (equal to that in the lasing state) was found to be 210, 280, 370, and 560 mW, for T = 0.5, 1, 2, and 3%, respectively.

As shown in Fig. 3 the laser efficiency was found to saturate for incident pump powers higher than 6 W. However, this is attributed mainly to the variation of the central pump wavelength and the broadening of the emission spectrum of the diode laser module. Fig. 5 shows the emission spectra of the diode laser module for three different power levels in comparison with the absorption cross section. One can see that, at the highest power level of 6.8 W, there is a substantial amount of power emitted beyond 980 nm while the optical absorption of Yb:NaLaW decreases rapidly for wavelengths exceeding 980 nm.

5. Conclusion

In summary, cw room temperature laser operation has been demonstrated with a disordered crystal of Yb:NaLaW for the first time with diode pumping. A maximum output power of 330 mW was achieved with an optical conversion efficiency of 4.9% and a slope efficiency of 6.3% with respect to the incident pump power. In terms of the absorbed pump power, however, the efficiencies are about three times higher. Yet higher output power levels and efficiencies are expected with improvement in the crystal optical quality and higher Yb-concentrations. In this work we also presented the refractive index dispersion curves for undoped NaLaW and some physical properties of NaLaW which are sensitive to the Yb

concentration and the polarization.

References

[1] Peterson GE, Bridenbaugh PM. Appl. Phys. Lett. 1964; 4: 173.

[2] Méndez-Blas A, Rico M, Volkov V, Cascales C, Zaldo C, Coya C, Kling A, Alves LC. J. Phys.: Condens. Matter 2004; 16: 2139.

[3] Rico M, Liu J, Griebner U, Petrov V, Serrano MD, Esteban-Betegón F, Cascales C, Zaldo C. Opt. Exp. 2004; 12: 5362.

[4] Johannsen J, Mond M, Petermann K, Huber G, Ackermann L, Rytz D, Dupre C. Advanced Solid-State Photonics 2005, paper MB44, Feb.6-9, Vienna, Austria, Technical Digest (CD-ROM).

[5] Liu J, Cano-Torres JM, Cascales C, Esteban-Betegón F, Serrano MD, Volkov V, Zaldo C, Rico M, Griebner U, Petrov V. phys. stat. sol. (a) 2005; 202: R29.

[6] Serrano MD, Esteban-Betegón F, Zaldo C. J. Cryst. Growth 2005; 275: e819.

[7] Mokhosoev MV, Krivobok VI, Aleikina SM, Zhigulina NS, Kisel' NG. Inorg. Mat. 1967; 3: 1444 (transl. from Izv. Akad. Nauk SSSR, Neorg. Mater. 1967; 3: 1657)

[8] Rode EYa, Karpov VN, Ivanova MM, Russ. J. Inorg. Chem. 1971; 16: 905 (transl. from Zhur. Neorg. Khim. 1971; 16: 1713).

[9] Byrappa K, Jain A. J. Mater. Res. 1996; 11: 2869.

[10] Gizhinskii AR, Bryzgalov IA, Gribina IA. Inorg. Mat. 1972; 8: 1957 (transl. from Izv. Akad. Nauk SSSR, Neorg. Mater. 1972; 8: 2219).

[11] Haumesser PH, Gaumé R, Viana B, Antic-Fidancev E, Vivine D, J. Phys.: Condens. Matter 2001; 13: 5427.

[12] Subbotin KA, Zharikov EV, Smirnov VA. Opt. Spectr. 2002; 92: 601 (transl. from

Optika i Spektroskopiya 2002; 92: 657).

[13] Liu J, Rico M, Griebner U, Petrov V, Peters V, Petermann K, Huber G. phys. stat. sol. (a) 2005; 202 : R19.

[14] Griebner U, Liu J, Rivier S, Aznar A, Grunwald R, Sole RM, Aguiló M, Díaz F, Petrov V. IEEE J. Quantum Electron. 2005; 41: 408.

Figure Captions

Fig. 1 Refractive indices of NaLa(WO$_4$)$_2$ measured at 300 K (symbols) and the corresponding

Sellmeier fits (curves).

Fig. 2 Schematic of the Yb:NaLa(WO$_4$)$_2$ laser end-pumped by a fiber-coupled diode laser

module.

Fig. 3 Output power versus incident pump power of the cw Yb:NaLa(WO$_4$)$_2$ laser for

different output couplers. The lines correspond to the linear fits used to estimate the slope

efficiency η.

Fig. 4 Variation of the Yb:NaLa(WO$_4$)$_2$ crystal absorption without lasing versus incident

pump power.

Fig. 5 Ground state optical absorption cross sections σ_{GSA} of Yb:NaLaW (a) and comparison

of the emission spectra of the diode laser module for different output levels (b).

Fig. 1. (by J. Liu et al.)

Focusing Optics

Laser Crystal
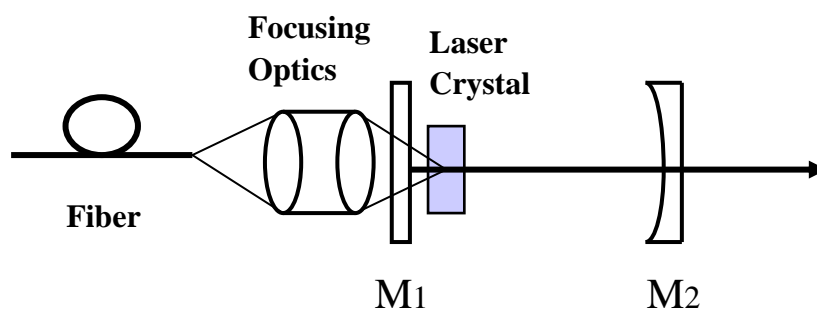
Fiber

M$_1$

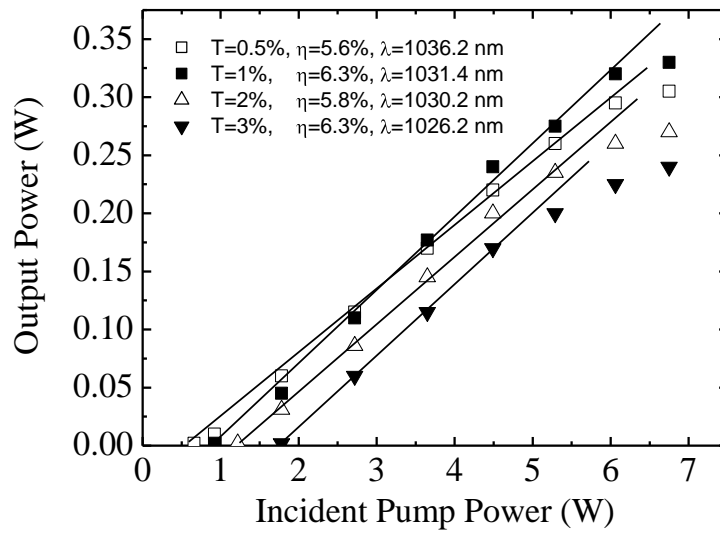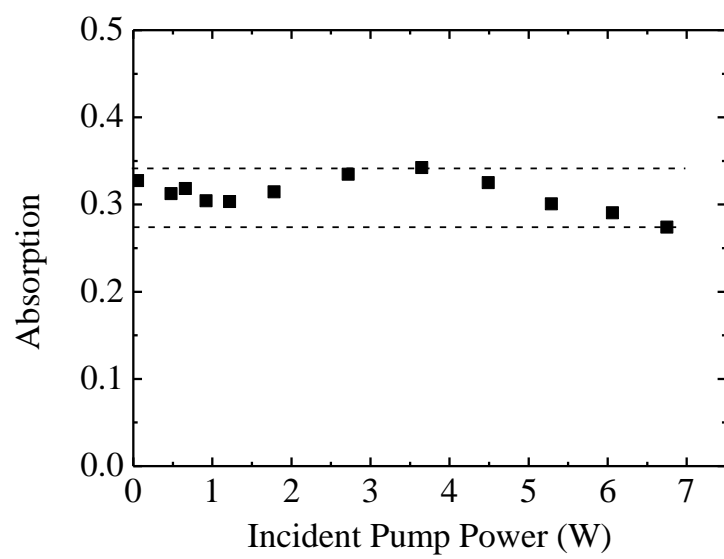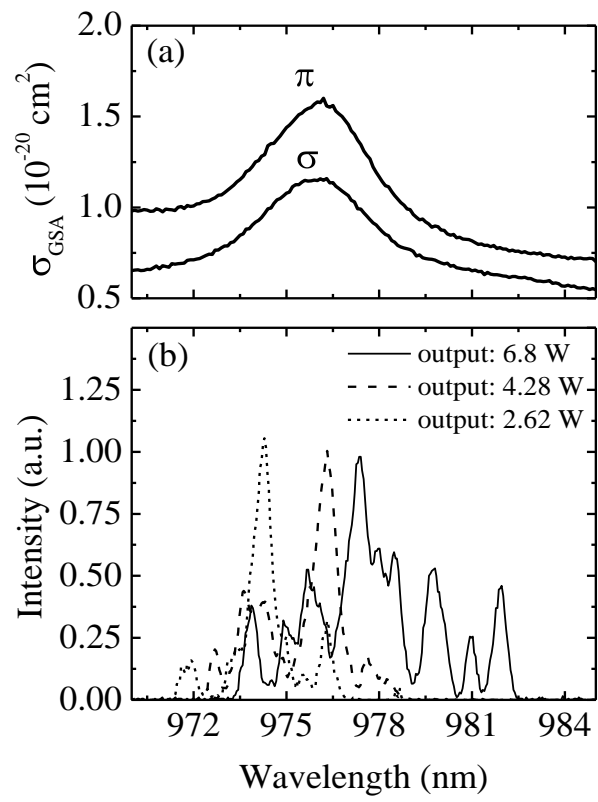M$_2$
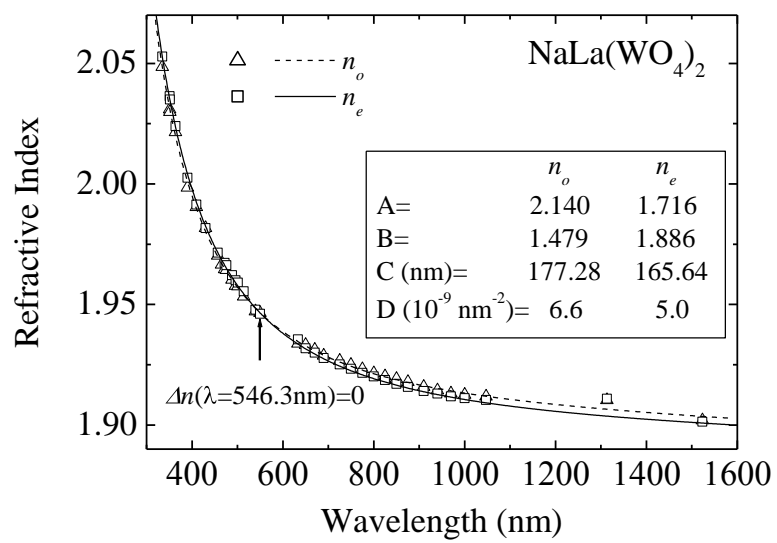
Fig. 2   (by J. Liu et al.)

Fig. 3   (by J. Liu et al.)

Fig. 4 (by J. Liu et al.)

Fig. 5 (by J. Liu et al.)